

Article

Not peer-reviewed version

Beyond Nano-Delivery: Synerjet-Assisted Transdermal Delivery of Nano-Formulated Nicotinamide Mononucleotide (Nano-NMN) for Comprehensive Skin Rejuvenation

[Wonkyu Hong](#)*, Jaewoo Kim, Seongmin Noh, [Joonho Shim](#), Seok-Kwang Park, [Mi-Hwa Kim](#)*

Posted Date: 7 May 2026

doi: 10.20944/preprints202605.0301.v1

Keywords: nicotinamide mononucleotide (NMN); Synerjet; skin rejuvenation; anti-aging; electroporation; nanoparticle; transdermal delivery; cold plasma; needle-free injector; microjet



Preprints.org is a free multidisciplinary platform providing preprint service that is dedicated to making early versions of research outputs permanently available and citable. Preprints posted at Preprints.org appear in Web of Science, Crossref, Google Scholar, Scilit, Europe PMC, OpenAlex.

Copyright: This open access article is published under a [Creative Commons CC BY 4.0 license](#), which permit the free download, distribution, and reuse, provided that the author and preprint are cited in any reuse.

Disclaimer/Publisher's Note: The statements, opinions, and data contained in all publications are solely those of the individual author(s) and contributor(s) and not of MDPI and/or the editor(s). MDPI and/or the editor(s) disclaim responsibility for any injury to people or property resulting from any ideas, methods, instructions, or products referred to in the content.

Article

Beyond Nano-Delivery: Synerjet-Assisted Transdermal Delivery of Nano-Formulated Nicotinamide Mononucleotide (Nano-NMN) for Comprehensive Skin Rejuvenation

Wonkyu Hong ^{1,*}, Jaewoo Kim ¹, Seongmin Noh ², Joonho Shim ², Seok-Kwang Park ³ and Mi-Hwa Kim ^{3,*}

¹ Class One Clinic, 10F, 390, Mijin Plaza, Gangnam-daero, Gangnam-gu, Seoul, 06232, Republic of Korea

² Benjamin Clinic, 6F, 138, Dosan-daero, Gangnam-gu, Seoul, 06037, Republic of Korea

³ Hironic. Co., Ltd., 19F, 767, U-Tower, Sinsu-ro, Suji-gu, Yongin, Gyeonggi-do, 16827, Republic of Korea

* Correspondence: mhkim1@hironic.com (M.-H.K.); hwk0417@gmail.com (W.H.);
Tel.: +82-31-525-7513 (M.-H.K.); +82-02-6958-8906 (W.H.)

Abstract

This study aimed to evaluate whether the Synerjet system can maximize the transdermal delivery and skin rejuvenation of nano-NMN. In a 4-week split-face trial (n=21), this combination demonstrated marked clinical superiority over topical nano-NMN alone ($p < 0.001$), yielding enhanced improvements in wrinkles (170.56% in periorbital and 154.45% in nasolabial, respectively), pore volume (176.62%), and deep hydration (188.02%). Regarding dermal integrity, the test group showed a 111.56% superior increment in skin elasticity and a 149.75% more effective optimization of melanin intensity. Notably, deep-tissue hydration at a 2.5 mm depth demonstrated a 188.02% higher gain, suggesting that the modality significantly fortifies the skin's physiological moisture reservoir. The test group exhibited a marked improvement over the control across all cutaneous parameters ($p < 0.001$). Our findings demonstrate that a new combinatorial approach using EP-assisted microjet of Synerjet system after cold plasma pretreatment and a nano-NMN 10% ampoule resulted in significantly greater improvements in wrinkles, pores, elasticity, pigmentation, and deep skin hydration compared to topical application alone. Consequently, these results demonstrated that Synerjet system effectively overcome the inherent limitations of nano-delivery technologies, offering a promising modality for advanced cutaneous rejuvenation and a robust framework for future professional dermatological treatments.

Keywords: nicotinamide mononucleotide (NMN); Synerjet; skin rejuvenation; anti-aging; electroporation; nanoparticle; transdermal delivery; cold plasma; needle-free injector; microjet

1. Introduction

Skin aging is driven by both intrinsic chronological processes and extrinsic factors, particularly photoaging induced by ultraviolet (UV) radiation. These processes result in clinically observable changes, including wrinkle formation, decreased elasticity, pigmentation, enlarged pores, and reduced skin hydration [1].

At the molecular level, a decline in nicotinamide adenine dinucleotide (NAD⁺) has been identified as a key contributor to aging. Reduced NAD⁺ levels are associated with impaired cellular energy metabolism, increased oxidative stress, and activation of pro-inflammatory pathways [2–11]. Nicotinamide mononucleotide (NMN), a critical intermediate in the NAD⁺ salvage pathway, restores intracellular NAD⁺ levels and mitigates age-related functional decline [12]. Recent dermatological

studies revealed NMN promotes collagen synthesis in dermal fibroblasts, reduce UV-induced wrinkle formation, and enhance skin hydration through upregulation of hyaluronic acid synthases (HAS-1 and HAS-2) [13]. Furthermore, β -NMN has demonstrated inhibitory effects on MAPK signaling pathways (ERK, JNK, and p38) and matrix metalloproteinase-1 (MMP-1) expression in UV-B-induced photoaging models, thereby attenuating collagen degradation [13]. Despite these promising biological effects, achieving sufficient delivery to deeper skin layers remains a major challenge by its hydrophilic nature and low permeability across the stratum corneum. To address this limitation, nano-formulation strategies and device-based penetration enhancement techniques have been explored to improve the clinical efficacy of bioactive compounds such as NMN and EGF [14–16].

To address the above challenges, the Synerjet system has been developed as a multimodal beauty medical device that synergistically integrates microjet injection, electroporation, and cold plasma technologies: First, cold plasma is utilized as a fundamental pre-treatment cleansing step to eliminate surface impurities and optimize the physiological environment of the skin prior to the primary procedure, thereby ensuring an ideal substrate for subsequent product application [17–19]. Second, microjet injection enables needle-free delivery of active compounds into the dermis at high velocity [20]. Lastly, to further enhance cellular uptake, electroporation is strategically employed to ensure the uniform distribution of residual formulations, such as nano-NMN [21]. By delivering precisely controlled, short electrical pulses, this modality transiently induces the formation of aqueous micropores within the lipid bilayer of cellular membranes. This temporary reduction in barrier integrity significantly lowers transdermal resistance, thereby facilitating the consistent transport of active ingredients into target tissues [21]. Based on these mechanisms, the Synerjet system distinguishes itself from conventional microjet-only devices capable of cosmetic jetting. This device allows for optimized transdermal delivery while preventing the risks associated with the unregulated penetration of cosmetic ingredients into the deeper dermal layers, a common safety concern in non-medical jetting systems.

In this study, we hypothesized that the combination of cold plasma-assisted skin preparation and EP-tip-coupled spray delivery may improve both the uniformity of topical application and the penetration efficiency of nano-NMN. To evaluate the efficacy and safety of a nano-NMN delivered using the Synerjet system under cosmetic-use conditions, a split-face design was adopted to enable intra-individual comparison between conventional topical application (left side) and device-assisted application (right side). Outcome evaluation was performed using non-invasive, cosmetic-oriented assessment parameters, including wrinkle appearance (periorbital and nasolabial areas), pore appearance, skin elasticity, pigmentation (intensity and area), and skin hydration levels.

2. Materials and Methods

2.1. Characteristics of the Test Product and Full Ingredient Disclosure

The nano-NMN 10% ampoule is a milky and slightly turbid water-based formulation containing NMN (99.9% purity), ensuring safety for long-term use and systemic absorption (Table A1). The full list of ingredients (INCI names) is available in Table A2. This product was supplied from DEFY NUMBER Co., Ltd.

2.2. Skincare Protocol: Sequential Cold Plasma and Electroporation

To maximize the skin-conditioning effects of nano-formulated NMN, a standardized skincare protocol was performed using the Synerjet device (SYNERJET PRO™, Hironic, Gyeonggi-do South Korea) [22]. This multi-functional beauty platform integrates cold plasma, electroporation (EP), and microjet technologies. For this study, a 10 mm EP tip was coupled with the microjet nozzle to allow for the simultaneous application of the serum and electrical stimulation (Figure 1). To ensure consistency across all participants, all procedures were conducted under uniform operating conditions and controlled environments throughout the study.

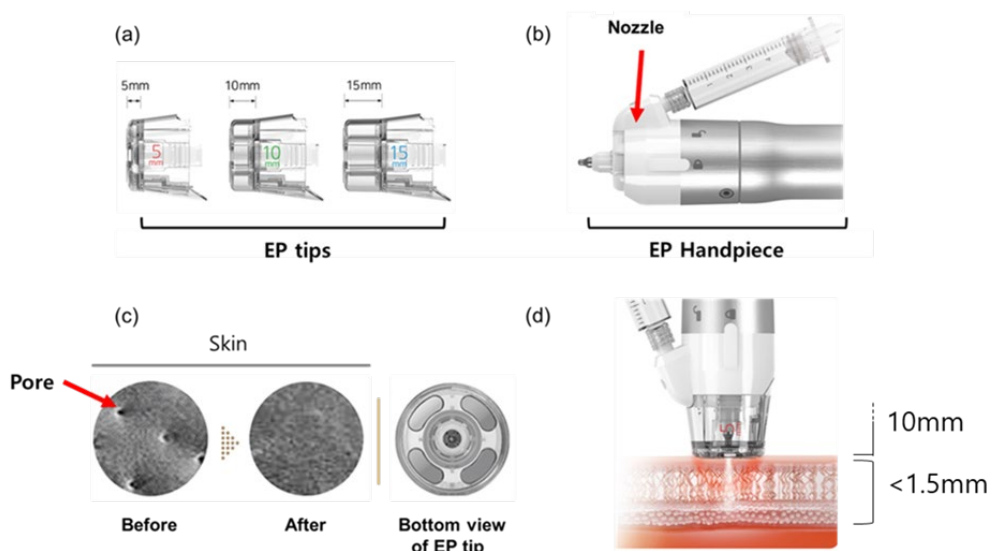


Figure 1. Schematic representation of the electroporation tips (EP Tips) and EP handpiece. (a) Three distance-controlled EP tips (5,10, and 15 mm) for tailored treatments. (b) The shape of EP nozzle and syringe attached handpiece (c) Representative images of skin surface before and after treatment, along with the structural design of the EP tip (d) Schematic illustration of the EP device in use, demonstrating EP-tip-coupled spray mode and plasma-rubbing mode.

2.2.1. Cold Plasma Skin Preparation

Prior to applying the active ingredients such as nano-NMN 10% ampoule, the skin surface was generally pre-conditioned with cold plasma in continuous mode (single pass). This preparatory step was designed to refine the skin texture by removing surface impurities and enhancing the skin's surface energy. This process improves the skin's hydrophilicity, ensuring the optimal state to absorb topically applied cosmetic formulations.

2.2.2. Synergistic Microjet Spray and Electroporation

Immediately following the plasma preparation, a 2 mL dose of nano-NMN 10% ampoule was applied to the skin. The formulation was delivered via the microjet spray mode through the EP-integrated nozzle. To enhance the permeability of the stratum corneum, the EP function was operated concurrently (Settings: Level 1, 15 Hz, 150 V). As illustrated in Figure 1d, the microcurrents induce the formation of transient aqueous pathways on the skin surface, significantly facilitating the transdermal absorption of the NMN molecules.

2.3. Study Design and Application Protocol

A split-face design was used for intra-individual comparison. The right side of the face was assigned to the test group (nano-NMN 10% ampoule + Synerjet), while the left side served as the control group (topical nano-NMN 10% ampoule). In the test group, Synerjet treatment was applied once weekly for four weeks, whereas in the control group, the ampoule was applied topically twice daily (morning and evening) over the same period (Table A1).

2.4. Study Participants (Subject) and Selection Criteria

A total of 21 healthy Korean women aged 30 years and older (mean age: 61.76 ± 8.2 years) participated in this study (Figure A1). All participants exhibited visible signs of skin aging, including facial wrinkles, enlarged pores, reduced elasticity, and hyperpigmentation. Of the initial cohort, 21 participants completed the full study, with one exclusion (Participant No. 21) occurring at week 4 due to a protocol violation. The study was conducted following a rigorous screening process based on the inclusion and exclusion criteria [23]. Throughout the study period, participants were strictly

instructed to maintain their existing skincare routines without introducing new products or medications (e.g., aspirin, antihistamines, or steroids). Additionally, excessive UV exposure from activities such as hiking or prolonged travel was restricted to ensure the stability of the experimental results.

2.5. Ethical Considerations

The study was conducted at the Human Skin Clinical Trials Center in strict accordance with the Good Clinical Practice (GCP) guidelines and the regulations established by the Ministry of Food and Drug Safety (MFDS). All procedures followed the institution's standard operating procedures (SOPs). The study protocol was reviewed and approved by the Institutional Review Board (IRB Approval No.: HM-IRB-P25-0510; Study Management No.: HM-P25-0510). The trial was commissioned by DEFY NUMBER Co., Ltd. and carried out from June 25 to July 24, 2025 [23].

2.6. Instrumental Skin Analysis and Evaluation

All measurements and evaluations were performed at baseline (before use) and after 4 weeks of product use using the appropriate instrument in a controlled environment without direct sunlight or air flow, under constant temperature and humidity conditions (22 ± 2 °C, $50\pm 5\%$ relative humidity). Participants were allowed to acclimate prior to assessment. Facial skin parameters were assessed using non-invasive instrumental methods. Wrinkle depth (periorbital and nasolabial regions), skin texture, pore volume (mm^3), erythema, and pigmentation were evaluated using Antera 3D[®] (Miravex Ltd., Dublin, Ireland) before and after treatment [24,25].

2.6.1. Wrinkle Depth

Wrinkle depth (mm) for two anatomical sites—periorbital (crow's feet) and nasolabial fold—was quantified using Antera 3D[®] at baseline (Day 0) and after 4 weeks of treatment (Day 28). The same facial landmarks and imaging settings were maintained to ensure consistency across both time points.

2.6.2. Pore Analysis

Images of the cheek area were captured using Antera 3D[®] imaging (Miravex Ltd., Dublin, Ireland) under standardized lighting conditions before and after four weeks of product application. Subsequently, the mean pore area (mm^2), pore density (ea/cm^2), mean pore volume (10^{-3}mm^3), total pore volume (mm^3), and maximum pore depth (mm) were measured in the cheek area at baseline and after treatment. Images were captured at identical facial regions, and proprietary software provided numerical outputs for each parameter.

2.6.3. Deep Skin Hydration

Deep skin hydration was assessed using a MoistureMeter D[®] (Delfin Technologies Ltd., Kuopio, Finland), which measures the tissue dielectric constant (TDC). Measurements were obtained at depths of 0.5, 1.5, 2.5, and 5.0 mm depths using XS5, S15, M25, and L50 probes [25]. Prior to each measurement session, the probe was calibrated according to the manufacturer's protocol. Three consecutive readings were obtained at each depth per subject, and the average value was recorded.

2.6.4. Pigmentation and Hyperpigmentation

DermaVision (Opto Biomed Co., Ltd., Gyeonggi-do, Republic of Korea) is a digital camera-based imaging system designed to capture frontal and lateral (left/right) views of the face. In this study, frontal facial images were captured in CPI (Cross-Polarized Image) mode before and after four weeks of product application. Subsequently, the melanin color (%) of the cheek area was comparatively analyzed using specialized analysis software. Hyperpigmented areas were quantified by measuring the melasma area (mm^2) using Antera 3D[®] imaging. Skin pigmentation was additionally analyzed

using DermaVision (Opto Biomed Co., Ltd., Gyeonggi-do, Republic of Korea) under cross-polarized imaging to determine melanin index (%) [26,27].

2.6.5. Skin Elasticity

Using the Cutometer® dual MPA 580 (Courage+ Khazaka Electronic GmbH, Cologne, Germany) with a 2 mm probe, the R2 (gross elasticity) values of the cheek area were measured and compared before and after four weeks of product use. The measurement involved applying negative pressure three times to the skin to evaluate the deformation and recovery cycles [28].

2.7. Compliance Assessment, Satisfaction Surveys, and Adverse Skin Reactions Assessment

Upon completion of the study, self-reported diaries were collected from the participants to evaluate their compliance. Participants with a compliance rate of less than 80.00% were excluded from the final analysis (Table A4). Following treatment, participants provided subjective assessments based on a questionnaire surveys provided by the sponsor. The evaluation was conducted using a 6-point Likert scale: 1 (Strongly disagree), 2 (Disagree), 3 (Slightly disagree), 4 (Slightly agree), 5 (Agree), and 6 (Strongly agree). Scores ranging from 4 to 6 were categorized as positive responses. Throughout the study period, the investigator monitored the occurrence of adverse skin reactions and the use of concomitant cosmetics use that may potentially affect the study results. In the event of an adverse reaction, the investigator immediately notified the Principal Investigator (PI). Following a thorough clinical assessment and appropriate medical intervention, the PI determined whether the participant could safely continue their participation in the study.

2.8. Statistical Analysis

Statistical analyses were performed using IBM SPSS Statistics 26 (SPSS Inc., Chicago, IL, USA) to verify the statistical significance of changes before and after product use. Statistical significance was defined as a p-value < 0.05 with a 95% confidence interval. Continuous variables derived from instrumental evaluations were expressed as mean±standard deviation (SD), while categorical variables from questionnaire assessments were presented as frequencies and percentages (%). The normality of the data distribution was verified using the Shapiro-Wilk test. For data measured at two time points, a paired t-test (parametric) was used if the normality assumption was met; otherwise, the Wilcoxon signed-rank test (non-parametric) was applied. For comparisons between groups, raw data were analyzed. A repeated measures ANOVA was employed for normally distributed data, while the Generalized Estimating Equation (GEE) was used for data that did not satisfy the normality assumption.

2.9. Calculation of Improvement Rate

The rate of improvement (%) for each parameter was calculated using the following formulas:

2.9.1. Percentage Improvement (Within-Group)

This formula assesses the rate of change within each group (test or control) before and after product use.

$$\text{Improvement Rate (\%)} = \frac{[\text{Value_Post} - \text{Value_Pre}]}{[\text{Value_Pre}]} \times 100$$

- **Value_pre** : Measurement before product use (Baseline)
- **Value_post** : Measurement after 4 weeks of product use

2.9.2. Improvement Rate Relative to the Control Group

This formula compares the efficacy of the test group (nano-NMN 10% Ampoule + Synerjet) against the control group (nano-NMN 10% Ampoule alone).

$$\text{Improvement Rate Relative to the Control Group (\%)} = \frac{[\text{Value}_T - \text{Value}_C]}{[\text{Value}_C]} \times 100$$

- **Value_T** : Measured value of the test group (treatment side)
- **Value_C** : Measured value of the control group (control side)

3. Results

A total of 21 healthy Korean participants were enrolled for this study based on the inclusion and exclusion criteria [23]. One participant(No.21) was withdrawn at fourth week due to a protocol violation. The mean age of the participants was 61.76±8.2 years old, range 47 to 73 (Figure A1). During this experiment, no patients reported side effect or intolerable pain requiring additional pain relief with analgesia or sedation. Patients were able to return to their usual activity immediately after treatment. Based on the combined effects of electroporation-facilitated delivery of nano-NMN and cold plasma-mediated skin preparation (Figure 1), significant improvements in multiple skin parameters were observed following treatment.

3.1. Assessment of Facial Wrinkles and Pore Volume

In advance, this study was conducted to evaluate the efficacy of the combinatorial approach in improving facial wrinkles (the periorbital, nasolabial regions) and pore volume (Table 1, Figure 2). These areas are among the earliest and most prominently affected by intrinsic and extrinsic skin aging, and therefore serve as reliable indicators for assessing the anti-aging performance of topical cosmetic products. After 4 weeks of use, both groups showed a significant reduction in eye wrinkle depth and nasolabial fold depth compared to baseline ($p < 0.05$). For eye wrinkles, the test group demonstrated a 10.37% improvement compared to 3.83% in the control group, with a significant difference between the two groups ($p < 0.001$). Similarly, nasolabial folds improved by 10.93% in the test group, significantly outperforming the control group's 4.29% improvement ($p < 0.001$). Pore volume also decreased significantly in both groups ($p < 0.001$), but the test group showed a much higher reduction rate (18.19%) compared to the control group (6.57%), indicating a statistically superior efficacy ($p < 0.001$). The improvement rates in the test group were markedly higher than those in the control group — specifically 170.56% higher for eye wrinkles and 154.45% higher for nasolabial folds ($p < 0.001$). The impact of the combination on skin texture was further evaluated through a quantitative analysis of pore volume in the cheek area (Table 1). Enlarged pores are a primary aesthetic concern often associated with age-related skin laxity and sebum dynamics. Therefore, a reduction in pore volume serves as a significant indicator of improved skin rejuvenation. As shown in Table 1, both the test and control groups demonstrated a reduction in mean pore volume following 4 weeks of application. In the test group, the mean pore volume decreased significantly from 0.0023±0.0012 at baseline to 0.0019±0.0012 at the 4-week ($p < 0.001$). For the control group, the pore volume changed from 0.0020±0.0007 to 0.0019±0.0007 during the same period ($p < 0.001$). While both groups exhibited improvements, the test group showed a substantial 18.19% reduction in visible pore appearance from baseline. This improvement was more than double the 6.57% reduction observed in the control group. These findings suggest that the synergistic application of the test formulation and delivery technology provides a clinically meaningful benefit in minimizing the appearance of pores and enhancing overall skin topography. Interestingly, a comparative analysis between the two groups revealed that the test group's efficacy in refining pore volume was markedly

superior. The test group exhibited a 176.62% higher improvement rate relative to the control group. The difference in the degree of change between the groups was statistically significant ($p < 0.001$, GEE), indicating that the synergistic effect of NMN and the Synerjet system provides a potent solution for minimizing the visible appearance of enlarged pores and enhancing overall skin smoothness.

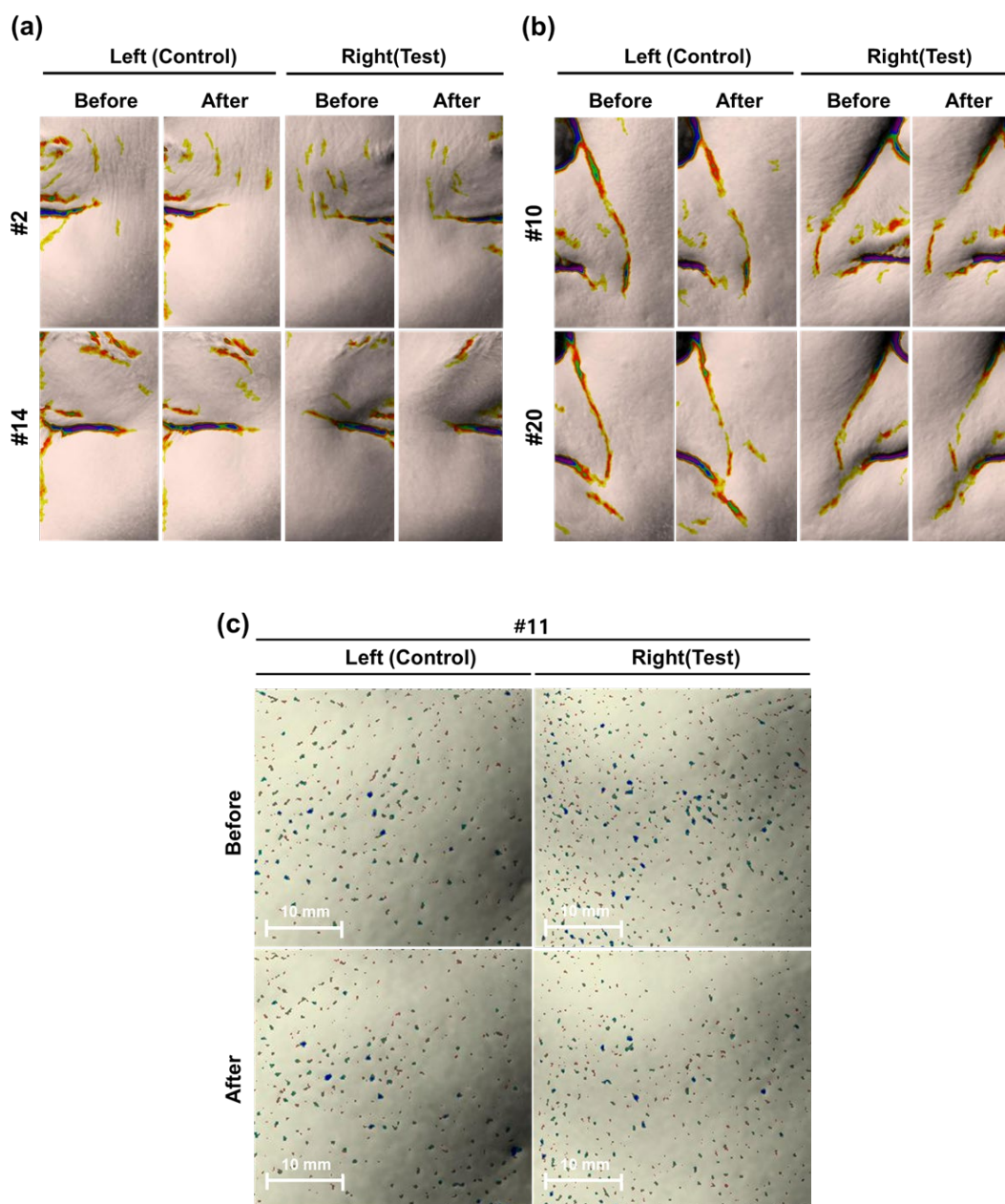


Figure 2. Antera 3D® Visual analysis of skin wrinkle and pore improvement before and after treatment. Representative skin surface images of five subjects (#2, #14, #10, #20, and #11) comparing the control (Left) and test (Right) groups. (a, b) Color-mapped topographic images illustrating wrinkle depth and distribution. A comparison between 'Before' and 'After' time points shows a more pronounced reduction in wrinkle intensity and area in the test group compared to the control group. These images demonstrate the visual efficacy of the treatment in improving skin texture and reducing the appearance of fine lines. (c) Comparative skin surface images of the control (Left) and test (Right) sites before and after treatment. The blue, green, and red markers indicate the distribution of pores, pigmentation, or skin blemishes identified by the imaging system. A reduction in the density and visibility of these markers is observed in the test group following treatment, demonstrating the skin-refining and clarifying efficacy of the test group compared to the control. Scale bars represent 10 mm.

Table 1. Measurements of wrinkles and pores before and after 4 weeks of application.

Parameter	Group	Baseline	After 4 weeks	Improvement rate (%)		Intra-group (p-value)	Inter-group (p-value)
				Treatment vs Baseline	Test vs Control		
Eye wrinkles (Average depth, mm)	Test	0.1009 ± 0.0422	0.0904 ± 0.0373	10.37%	170.56%	<0.001	<0.001
	Control	0.0927 ± 0.0366	0.0891 ± 0.0347	3.83%		<0.001	
Nasolabial folds (Average depth, mm)	Test	0.0830 ± 0.0203	0.0739 ± 0.0184	10.93%	154.45%	<0.001	<0.001
	Control	0.0769 ± 0.0186	0.0736 ± 0.0186	4.29%		0.001	
Pore volume (mm ³)	Test	0.0023 ± 0.0012	0.0019 ± 0.0012	18.19%	176.62%	<0.001	<0.001
	Control	0.0020 ± 0.0007	0.0019 ± 0.0007	6.57%		<0.001	

3.2. Assessment of Skin Elasticity and Pigmentation

To further evaluate the comprehensive anti-aging effects of the combinatorial approach, we analyzed changes in skin elasticity (R2 value) and pigmentation parameters, including melanin color intensity and the total area of hyperpigmentation (Table 2, Figure 3). Skin elasticity (R2 value) significantly increased in both the test and control groups after 4 weeks ($p < 0.001$). The test group showed a 2.88% increase in the R2 value, which was a 111.56% greater improvement relative to the control group (1.36%). Regarding skin tone uniformity, the test group showed a substantial decrease in melanin color intensity (19.35%) and a significant reduction in the total area of hyperpigmentation (25.49%). In contrast, the control group showed a 7.75% and 13.34% reduction, respectively. As shown in Figure 3, the synergistic protocol demonstrated a markedly more pronounced reduction in both pigmentation density and localized dyschromia compared to the topical-only control. Representative clinical imaging (Figure 3a, Right) using Antera 3D[®] revealed that hyperpigmented lesions (indicated by yellow arrows) underwent significant contraction in surface area and a visible attenuation of melanin intensity following the four-week intervention. These clinical observations were further validated by DermaVision topographic heatmap analysis (Figure 3b). The test group exhibited a distinct transition from high-intensity “hot spots” (red/yellow) to more homogenous, neutralized zones (green/blue), signifying a substantial enhancement in skin tone uniformity. Conversely, the control group (Figure 3b, Left) showed only marginal alterations in pigment distribution, underscoring the inherent limitations of topical application regarding transdermal penetration. The superior clearance of epidermal pigments in the test group suggests that the sequential integration of cold plasma and electroporation (EP)-coupled microjet propulsion significantly optimized the transdermal flux of the nano-formulated NMN complex. This physico-mechanical synergy likely accelerated the turnover of pigmented keratinocytes while facilitating the deep-tissue delivery of active depigmenting agents, such as niacinamide. Notably, quantitative analysis confirmed the protocol’s efficacy, with the test group exhibiting a 149.75% higher improvement in melanin color and a 91.14% greater reduction in hyperpigmented areas compared to the control ($p < 0.001$). Collectively, these visual and quantitative assessments confirm that the combinatorial platform offers a superior clinical advantage in correcting visible skin irregularities. The integration of these advanced delivery modalities represents a highly effective strategy for maximizing the functional performance of cosmeceuticals in treating complex dermal pigimentary concerns.

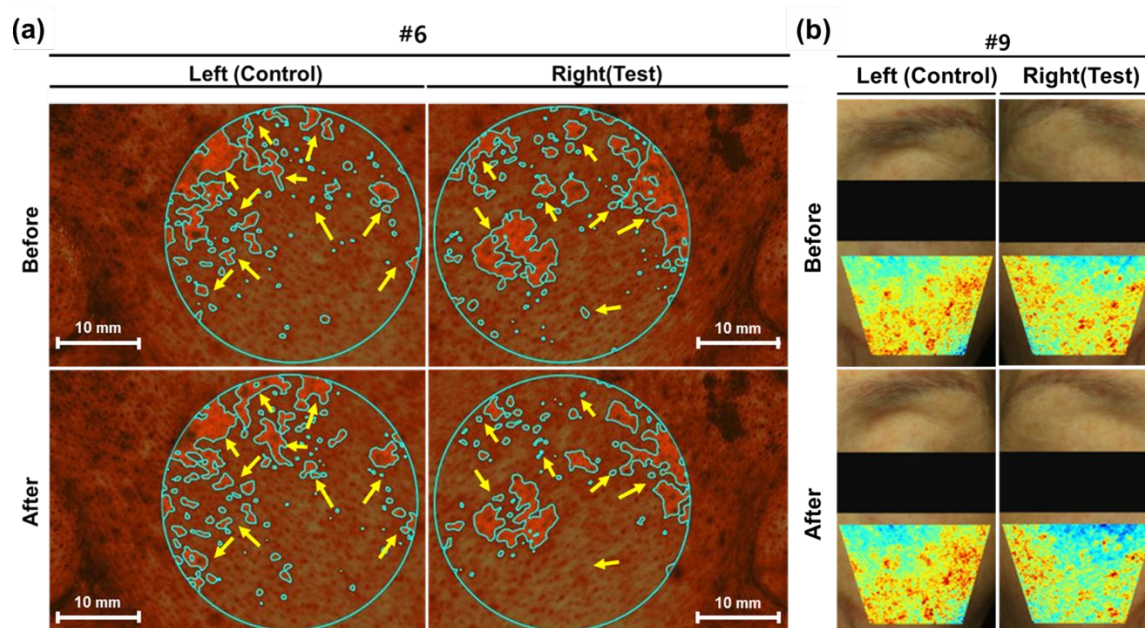


Figure 3. Visual evaluation of skin tone and pigmentation improvement for subjects #6 and #9. Antera 3D® (a) and DermaVision (b) images of control (Left) and test (Right) groups before and after treatment. (a) Pigmentation and redness analysis for Subject #6. Mint-colored outlines and yellow arrows indicate targeted areas of hyperpigmentation. Both groups show a noticeable reduction in the size and intensity of these areas compared to the baseline (Before). (b) Skin tone uniformity analysis for Subject #9. The heatmaps represent the distribution of skin brightness or redness intensity. Following treatment, the test group displays more decrease than the control group in high-intensity red areas, indicating an improvement in overall skin tone evenness and radiance. Scale bars represent 10 mm.

Table 2. Measurement of skin elasticity and pigmentation.

Parameter	Group	Baseline	After 4 weeks	Improvement Rate (%)		Intra-group (p-value)	Inter-group (p-value)
				Treatment vs Baseline	Test vs Control		
Skin Elasticity (R2 value)	Test	0.6551 ± 0.0550	0.6740 ± 0.0567	2.88%	111.56%	<0.001	<0.001
	Control	0.6581 ± 0.0531	0.6670 ± 0.0548	1.36%		<0.001	
Melanin Color (%)	Test	50.53 ± 24.93	40.76 ± 23.03	19.35%	149.75%	<0.001	<0.001
	Control	42.91 ± 24.95	39.59 ± 24.99	7.75%		0.018	
Hyperpigmentation Area (mm ²)	Test	116.73 ± 21.86	86.98 ± 22.77	25.49%	91.14%	<0.001	<0.001
	Control	111.80 ± 23.73	96.90 ± 24.51	13.34%		<0.001	

3.3. Evaluation of Deep Skin Hydration (Tissue Dielectric Constant, TDC)

To evaluate the depth-dependent moisturizing efficacy of the EP-tip-coupled microjet of Synerjet system with cold plasma pre-treatment, TDC measurements were performed at four specific dermal depths: 0.5, 1.5, 2.5, and 5.0 mm. These measurements reflect the system's ability to modulate water content across different anatomical strata of the skin. As shown in Table 3, the test group demonstrated a robust and statistically significant increase in skin hydration at all measured depths up to 2.5 mm ($p < 0.001$). Following the 4-week intervention, the test group achieved improvement rates of 13.94% at 0.5 mm, 7.01% at 1.5 mm, and 5.74% at 2.5 mm. These values were markedly higher than those of the control group (8.21%, 3.81%, and 1.99%, respectively), highlighting a superior

capacity for moisture retention within the tissue. A comparative analysis of the improvement rates further underscores the system's efficiency; the test group exhibited a 69.80% higher improvement at 0.5 mm, an 83.94% increase at 1.5 mm, and a remarkable 188.02% higher efficiency at 2.5 mm compared to the control group ($p < 0.001$). These data indicate that the Synerjet system facilitates effective moisture delivery beyond the superficial stratum corneum, extending into the deeper epidermal and dermal layers. In contrast, no significant deviation from baseline was observed at the 5.0 mm depth for either group ($p > 0.05$), with no statistically significant difference between cohorts ($p = 0.192$). This results suggest that the Synerjet system's primary bio-stimulating and hydrating influence is optimally concentrated within the upper 2.5 mm of the skin tissue, where key regenerative processes and collagen-elastin matrices are located.

Table 3. Skin hydration at different depths.

Depth	Group	Baseline	After 4 weeks	Improvement rate (%)		Intra-group (p-value)	Inter-group (p-value)
				Treatment vs Baseline	Test vs Control		
0.5 mm	Test	42.89 ± 3.35	48.87 ± 4.20	13.94%	69.80%	<0.001	<0.001
	Control	42.31 ± 3.36	45.78 ± 4.15	8.21%		<0.001	
1.5 mm	Test	39.56 ± 3.65	42.33 ± 3.53	7.01%	83.94%	<0.001	<0.001
	Control	38.64 ± 3.58	40.11 ± 3.75	3.81%		<0.001	
2.5 mm	Test	33.45 ± 2.79	35.37 ± 2.89	5.74%	188.02%	<0.001	<0.001
	Control	33.11 ± 2.89	33.77 ± 2.94	1.99%		<0.001	
5.0 mm	Test	25.67 ± 2.32	25.73 ± 2.39	-		0.499	0.192
	Control	25.56 ± 2.48	25.48 ± 2.47	-		0.194	

3.4. Compliance, Safety Evaluation, and Participants-Reported Outcomes

Following the procedures in Table A3, 21 of participants completed a self-administered questionnaire that assessed their satisfaction with skin improvement on both sides of their faces and any side effects (Table 4). The study recorded a high participant compliance rate of 99.70% (Table A4), indicating strict adherence to the application protocol. The skin compatibility of the combination treatment was evaluated through continuous monitoring of skin responses and a 4-week post-application self-assessment. Overall, participants addressed high satisfaction with the combination treatment involving nano-NMN 10% ampoule and the EP-tip-coupled microjet spray mode of Synerjet following cold plasma pretreatment (Table A5). Participants were pre-screened for various skin conditions, including erythema, edema, scaling, pruritus, tingling, burning sensation, stiffness, and stinging. Although this study was conducted over a 4-week period, notable skin discomfort or irritation was not observed or reported on either side of the face throughout the study (Table 4). Considering that the 28-day study duration aligns with the natural epidermal turnover cycle, the absence of any cumulative irritation—such as scaling or chronic erythema—indicates that the nano-NMN 10% ampoule and device combination is well-tolerated. These findings indicate that the protocol is safe for sustained, routine daily use in a clinical or home-care setting.

Table 4. Evaluation of skin adverse reactions after 4 weeks of product application.

No	Adverse Skin Reaction	After 4 Weeks of Use
1	Erythema (Redness)	0
2	Edema (Swelling)	0
3	Scaling (Dead skin cells)	0
4	Pruritus (Itching)	0
5	Tingling (Pain)	0
6	Burning sensation	0
7	Stiffness	0
8	Stinging	0

Severity Scale; 0 - None; 1-Mild;; 2-Moderate; 3-Severe

4. Discussion

The growing interest in anti-aging and skin rejuvenation has driven considerable innovation at the intersection of cosmetic formulation science (Cosmeceuticals) and transdermal drug delivery technology [29,30]. In particular, the development of advanced permeation-enhancement platforms (including dissolving microneedles, biodegradable threads, ethosomes and liposomal carriers) reflects an industry-wide recognition that the biological efficacy of bioactive compounds is fundamentally constrained by the skin's barrier function [30,31]. In the context of, this study investigated whether a combinatorial approach integrating nano-NMN 10% ampoule with the Synerjet multi-functional delivery system could produce meaningful anti-aging outcomes superior to topical application alone.

NMN has attracted substantial scientific interest as a potent NAD⁺ precursor capable of restoring mitochondrial bioenergetics, DNA repair, and attenuating age-associated metabolic dysregulation [32]. The groundbreaking research by Sinclair et al., demonstrating that NMN supplementation is associated with increased telomere length, has further reinforced the conceptual framework that aging may be modifiable at the molecular level—a perspective that has catalyzed translational efforts in both pharmaceutical and cosmeceutical sectors [33–38]. Despite its promising biological profile, the clinical translation of NMN into topical cosmeceutical applications has historically been impeded by its pronounced hydrophilicity, which severely limits passive diffusion across the stratum corneum's lipophilic barrier. Nanoencapsulation—particularly liposomal and nanoparticle-based formulations—represented a critical first-generation solution, offering protection of the active ingredient from oxidative degradation and enabling enhanced partitioning into the lipid matrix of the stratum corneum [39–41]. Nevertheless, nanoparticle-based systems retain inherent limitations: the physical barrier of the stratum corneum cannot be fully overcome by particle size reduction alone, and premature cargo release prior to target-layer penetration remains a clinically relevant concern that constrains the intracellular bioavailability of NMN and, consequently, its capacity to elevate epidermal NAD⁺ concentrations to therapeutically meaningful levels [40–42].

Unlike conventional microjet-only devices that function primarily through subcision-mediated mechanical disruption, the Synerjet system is distinguished by its capacity to integrate cold plasma, electroporation (EP), and EP-tip-coupled microjet spray modalities within a single treatment workflow, operable via discrete SJ and PS handpieces either independently or in combination [22]. In the treatment protocol evaluated here, the PS handpiece's cold plasma function served a dual

preparatory role: surface decontamination and transient reorganization of intercellular lipid lamellae within the stratum corneum, thereby lowering the energetic barrier to nanoparticle penetration. Subsequently, EP-tip-coupled microjet delivery via the SJ handpiece facilitated uniform epidermal distribution of the nano-NMN formulation through a spray-based mechanism while the electroporation component generated transient aqueous pores within keratinocyte membranes, creating preferential pathways for deeper, more homogeneous nanoparticle infiltration [43]. Critically, the EP function optimized the surface charge of nanoparticles remaining within the stratum corneum, enhancing their affinity for epidermal cellular membranes and preventing transcutaneous efflux of active ingredient, thereby ensuring that NMN's physiological activity was sustained within the target tissue compartment.

The quantitative data presented in Table 1 demonstrate that while topical nano-NMN application alone produced statistically significant improvements in facial wrinkles (the periorbital and nasolabial regions) relative to intra-group baseline measurements, the Synerjet-augmented protocol yielded substantially superior outcomes across all skin parameters compared to the control group. These findings are mechanistically coherent, by preserving nanoparticle structural integrity during the delivery process while simultaneously ensuring target-layer localization of NMN, the Synerjet system maximized the intracellular NAD⁺ conversion rate in a manner that is unlikely to be achieved through passive topical delivery. The observed reduction in pore number and size, with concomitant improvement in skin elasticity, is consistent with NMN-mediated enhancement of dermal fibroblast metabolic activity [44]. Improvements in pigmentation irregularities, including melasma, are attributable to the niacinamide-driven suppression of melanocyte-keratinocyte melanosome transfer [36,45], while the enhancement in skin hydration reflects the depot-forming properties of the nine-component hyaluronic acid complex within the epidermis [46]. Collectively, these mechanisms constitute a well-defined anti-aging synergy that is critically dependent on adequate bioavailability of the active constituents at the target tissue level, a condition that the Synerjet delivery system was uniquely positioned to fulfill.

Among the 21 healthy female participants who completed the four-week intervention, no adverse events including pruritus, vesiculation, or inflammatory reactions were documented, indicating a favorable tolerability profile consistent with the keratinization cycle-matched treatment interval. Most participant satisfaction scores of 4 or above across the cohort further support the combined approach. It should be acknowledged, however, that the present study is limited by its relatively small sample size, the absence of histological or molecular validation of NAD⁺ upregulation, and the lack of a longer follow-up period to assess durability of observed improvements. Furthermore, the current protocol did not incorporate the Synerjet microjet function for intradermal delivery or subcision, which could have further enhanced collagen remodeling and improved the overall aesthetic outcome for deep-seated scars. Accordingly, future investigations should address these limitations and expand the mechanistic framework to include quantitative assessments of collagen synthesis rates, dermal matrix remodeling biomarkers, and the kinetics of skin regeneration following microjet-assisted NMN delivery, which will be essential for establishing the evidence base required for dermatological endorsement of this combinatorial platform.

5. Conclusions

Taken together, this four-week split-face study highlights the Synerjet system as a transformative platform for optimized transdermal delivery, achieving a remarkable 110–190% increase in efficacy ($p < 0.001$) for nano-NMN 10% compared to topical application. By integrating electroporation (EP) with precise jet technology, the system effectively overcomes the penetrative barriers of hydrophilic cosmetics while eliminating the safety risks of unregulated deep-dermal penetration often associated with conventional microjet-only devices. Moving forward, Synerjet system is poised to redefine the standards of non-invasive aesthetic medicine, offering a versatile and safe delivery engine for diverse high-molecular-weight actives such as peptides and exosomes.

Author Contributions: Conceptualization, Resources, methodology, formal analysis, investigation, data curation, validation, writing—original draft preparation, supervision, visualization, project administration, funding acquisition, WH. Resources, project administration, supervision, JK, SN & JS. Conceptualization, methodology, validation, writing—review and editing, SKP. Conceptualization, Resources, methodology, data curation, validation, writing—original draft preparation, visualization, project administration, MHK. All authors have read and agreed to the published version of the manuscript.

Funding: This research was funded by DEFY NUMBER Co., Ltd. and HIRONIC Co., Ltd.

Institutional Review Board Statement: The study was conducted at the Human Skin Clinical Trials Center in strict accordance with the Good Clinical Practice (GCP) guidelines and the regulations established by the Ministry of Food and Drug Safety (MFDS). All procedures followed the institution's standard operating procedures (SOPs). The study protocol was reviewed and approved by the Institutional Review Board (IRB Approval No.: HM-IRB-P25-0510; Study Management No.: HM-P25-0510). The trial was commissioned by DEFY NUMBER Co., Ltd. and carried out from June 25 to July 24, 2025 [23].

Informed Consent Statement: Not applicable.

Data Availability Statement: The data supporting the findings of this study are available from the corresponding author upon reasonable request.

Acknowledgments: Not applicable.

Conflicts of Interest: No conflicts to disclosure.

Abbreviations

The following abbreviations are used in this manuscript:

nano-NMN	Nano-formulated Nicotinamide Mononucleotide
TDC	Tissue Dielectric Constant
UV	Ultraviolet
HAS	Hyaluronic acid synthases
MMP-1	Matrix metalloproteinase-1
MFDS	the Ministry of Food and Drug Safety
IRB	the Institutional Review Board
GEE	Generalized Estimating Equation

Appendix A

Table A1. Characteristics of the test product and application protocol.

Parameter	Description
Product Name	Nano NMN 10% Ampoule
Formulation	Liquid
Test Product Control Number	250620-E-2
Number of Samples Received	123
Date of Receipt	20-Jun-25
Product Information	All relevant information regarding the test product was provided by the sponsor.
Analytical Evaluation	No chemical analyses were conducted to assess the stability or physicochemical properties of the test product.
Storage Conditions	Samples were stored at 5–25 °C, protected from heat and direct sunlight. All samples were retained for 180 days after issuance of the test report and discarded thereafter unless otherwise requested by the sponsor.
Application Site	Facial skin
Treatment Regimen	Test Group: 0.5 mL Nano NMN 10% Ampoule applied using a Synerjet device once weekly for 4 weeks
	Control Group: Applied twice daily (morning and evening) for 4 weeks according to individual routine
Application Procedure	The product was used following the sponsor's instructions: (1) after cleansing, toner was applied to completely dry skin; (2) the ampoule was sprayed approximately twice and evenly distributed over the face; (3) application was performed twice daily (morning and evening); (4) the skin was gently patted to enhance absorption.

Table A2. Full ingredient list for nano-NMN 10% ampoule (INCI names and functional classification).

Nano NMN 10% ampoule
Purified Water (solvent); Nicotinamide Mononucleotide (skin-conditioning agent); Glycerin (humectant); Caprylic/Capric Triglyceride (emollient); Butylene Glycol (humectant, solvent); Niacinamide (skin-conditioning agent); 1,2-Hexanediol (solvent, preservative booster); Polyglyceryl-10 Laurate (emulsifier); Hydrogenated Lecithin (emollient, emulsifier); Pentylene Glycol (humectant); Caprylyl Glycol (humectant, preservative booster); Xanthan Gum (thickening agent); Adenosine (skin-conditioning agent); Adipic Acid (pH adjuster); Sodium Hyaluronate, Hyaluronic Acid, Hydrolyzed Sodium Hyaluronate, Hydrolyzed Hyaluronic Acid, Hydrolyzed Glycosaminoglycans, Sodium Hyaluronate Crosspolymer, Sodium Acetylated Hyaluronate, Dimethylsilanol Hyaluronate, and Hydroxypropyltrimonium Hyaluronate (humectants and skin-conditioning agents).

Table A3. Schedule of assessments (SoA).

Assessments	Treatment					
	Baseline	After 1st	After 2nd	After 3rd	After 4th	After 4 Weeks
Informed consent obtained	Yes	No	No	No	No	Yes
Improvement of facial wrinkles (periorbital, nasolabial)	Yes	No	No	No	No	Yes
Pore improvement	Yes	No	No	No	No	Yes
Skin elasticity improvement	Yes	No	No	No	No	Yes
Improvement in pigmentation density	Yes	No	No	No	No	Yes
Improvement in pigmentation area	Yes	No	No	No	No	Yes
Improvement in deep skin hydration	Yes	No	No	No	No	Yes
Compliance evaluation	No	No	Yes	Yes	Yes	Yes
Questionnaire assessment	No	No	No	No	No	Yes
Adverse event evaluation	No	Yes	Yes	Yes	Yes	Yes

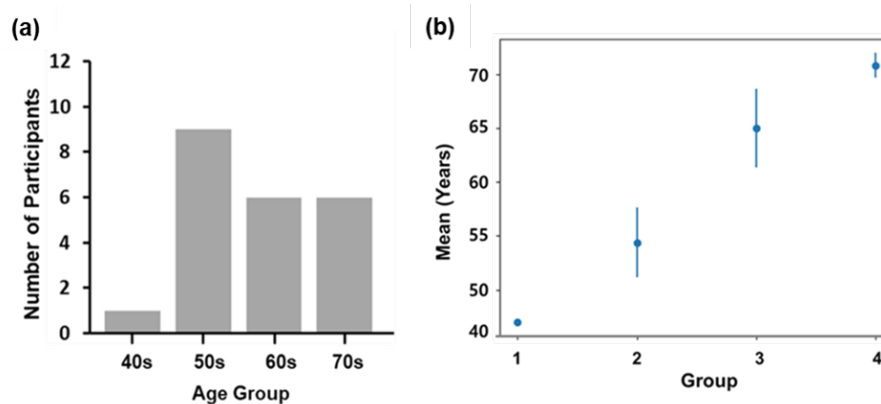


Figure A1. Age distribution of participants and mean age across groups. (a) Histogram representing the distribution of participants by age decade. The largest proportion of participants is in their 50s, while the smallest is in their 40s. (b) Mean age (years) for each of the four experimental groups (Groups 1–4). Data points represent the mean values.

Table A4. Compliance evaluation result data.

No.	Used twice a day (morning, evening) for 2 weeks.		
	Target Number of Uses	Actual Number of Uses	Compliance (%)
1	55	55	100
2	55	55	100
3	55	55	100
4	55	54	98.18
5	55	55	100
6	55	55	100
7	55	55	100
8	55	55	100
9	55	55	100
10	55	55	100
11	55	55	100
12	55	54	98.18
13	55	55	100
14	55	55	100
15	55	55	100
16	55	55	100
17	55	55	100
18	55	53	96.36
19	55	55	100
20	55	55	100
21	55	55	100
22	55	55	100
Mean	55	54.83	99.7

Table A5. Self-Assessment survey results.

No.	Survey Items (7-point Likert Scale)	1	2	3	4	5	6	7	8	9	10	11	12	13	14	15	16	17	18	19	22	21	20
1	Improvement in periorbital wrinkles	5	2	4	4	6	6	5	5	6	5	5	6	5	5	4	4	2	6	4	4		5
2	Improvement in nasolabial folds	4	2	4	4	6	6	5	4	6	4	5	6	5	5	3	4	2	6	4	4		4
3	Improvement in skin elasticity	4	4	5	4	6	6	5	6	6	5	6	6	4	5	4	4	2	6	5	4		6
4	Improvement in hyperpigmentation	4	5	5	4	6	6	5	6	6	4	5	6	3	5	3	4	2	6	5	3		5
5	Improvement in skin hydration	4	4	5	4	6	6	5	6	6	5	5	6	4	5	4	4	2	6	5	4		6
6	Satisfaction with product texture	5	5	5	4	6	6	5	6	6	4	6	6	6	5	4	4	1	6	5	4		5
7	Absorption of the product	4	6	5	4	6	6	5	6	6	5	6	6	6	5	4	5	2	6	5	4		5
8	Satisfaction with the fragrance	4	6	5	4	6	6	5	5	6	4	5	6	6	5	4	5	1	6	5	4		4
9	Intent to recommend to others	4	6	4	4	6	6	5	5	6	5	5	6	6	5	3	5	2	6	5	4		5
10	Overall product satisfaction	5	5	5	4	6	6	5	5	6	5	5	6	6	5	4	5	2	6	5	4		5
																						N/A	

References

1. Hussein, R.S.; Bin Dayel, S.; Abahussein, O.; El-Sherbiny, A.A. Influences on skin and intrinsic aging: Biological, environmental, and therapeutic insights. *J. Cosmet. Dermatol.* 2025, 24, e16688.
2. Fang, EF.; Lautrup, S.; Hou Y.; Demarest, TG.; Croteau, DL.; Mattson, MP.; Bohr, VA. NAD⁺ in Aging: Molecular Mechanisms and Translational Implications. *Trends Mol Med.* 2017, 23(10):899–916.
3. Verdin, E. NAD⁺ in aging, metabolism, and neurodegeneration. *NAD⁺ in Aging, Metabolism, and Neurodegeneration.* Science 2015, 350(6265), 1208–1213.
4. Covarrubias, A.J.; Perrone, R.; Grozio, A.; Verdin, E. NAD⁺ metabolism and its roles in cellular processes during ageing. *Nat. Rev. Mol. Cell Biol.* 2021, 22(2), 119–141.
5. Katsyuba, E.; Romani, M.; Hofer, D.; Auwerx, J. NAD⁺ homeostasis in health and disease. *Nat. Metab.* 2020, 2(1), 9–31.
6. Camacho-Pereira, J.; Tarragó, M.G.; Chini, C.C.S.; Nin, V.; Escande, C.; Warner, G.M.; Puranik, A.S.; Schoon, R.A.; Reid, J.M.; Galina, A.; et al. CD38 dictates age-related NAD decline and mitochondrial dysfunction through an SIRT3-dependent mechanism. *Cell Metab.* 2016, 23(6), 1127–1139.
7. Covarrubias, A.J.; Kale, A.; Perrone, R.; Lopez-Dominguez, J.A.; Oliveira Pisco, A.; Kasler, H.G.; Schmidt, M.S.; Heckenbach, I.; Kwok, R.; Wiley, C.D.; Wong, H.-S.; Gibbs, E.; Iyer, S.S.; Basisty, N.; Wu, Q.; Kim, I.-J.; Silva, E.; Vitangcol, K.; Shin, K.-O.; Lee, Y.-M.; Riley, R.; Ben-Sahra, I.; Ott, M.; Schilling, B.; Verdin, E. Senescent cells promote tissue NAD⁺ decline during ageing via the activation of CD38⁺ macrophages. *Nat. Metab.* 2020, 2(11), 1265–1283.
8. Novak EA.; Crawford EC.; Mentrup HL.; Griffith BD.; Fletcher DM.; Flanagan MR.; Schneider C.; Firek B.; Rogers MB.; Morowitz MJ.; Piganelli JD.; Wang Q.; Mollen KP. Epithelial NAD⁺ depletion drives mitochondrial dysfunction and contributes to intestinal inflammation. *Front Immunol.* 2023,14, 1231700.
9. Zhu, C.; Gu, H.; Jin, Y.; Wurm, D.; Freidhof, B.; Lu, Y.; Chen, Q.M. Metabolomics of oxidative stress: Nrf2 independent depletion of NAD or increases of sugar alcohols. *Toxicol. Appl. Pharmacol.* 2022, 442, 115949.
10. Pugel, A.D.; Schoenfeld, A.M.; Alsaifi, S.Z.; Holmes, J.R.; Morrison, B.E. The role of NAD⁺ and NAD⁺-boosting therapies in inflammatory response by IL-13. *Pharmaceuticals* 2024, 17(2), 226.
11. Schultz, M.B.; Bochaton, T.; Bonkowski, M.; Li, J.; Lokitiyakul, D.; Colville, A.; Gomes, A.; Sinclair, D. NAD⁺ depletion as a cause of inflammaging. *Innov. Aging* 2018, 2(Suppl. 1), 746.
12. Poljsak, B.; Milisav, I. NAD⁺ as the link between oxidative stress, inflammation, caloric restriction, exercise, DNA repair, longevity, and health span. *Rejuvenation Res.* 2016, 19(5), 406–415.
13. Kim, S.J.; Lee, S.; Choi, Y.J.; Kang, M.; Lee, J.; Hwang, G.S.; Roh, S.-S.; Jin, M.H.; Park, S.; Park, M.; Cho, H.S.; Kang, K.S. β -nicotinamide mononucleotide enhances skin barrier function and attenuates UV-B-induced photoaging in mice. *Antioxidants* 2025, 14(12), 1424.
14. Kessler, J.C.; Martins, I.M.; Manrique, Y.A.; Gudjónsdóttir, S.D.; Rodrigues, A.E.; Barreiro, M.F.; Dias, M.M. Microencapsulation of Epidermal Growth Factor (EGF) in Arabic Gum/Gelatine A Coacervates and Its Incorporation into Cosmetics: Evaluation of Skin Barrier Function and Ageing Indicators. *Cosmetics* 2026, 13(2), 89.
15. Musielak, E.; Krajka-Kuźniak, V. Liposomes and Ethosomes: Comparative Potential in Enhancing Skin Permeability for Therapeutic and Cosmetic Applications. *Cosmetics* 2024, 11(6), 191.
16. Jiang, X.; Zhao, H.; Li, W. Microneedle-Mediated Transdermal Delivery of Drug-Carrying Nanoparticles. *Front. Bioeng. Biotechnol.* 2022, 10, 840395.
17. He, R.; Li, Q.; Shen, W.; Wang, T.; Lu, H.; Lu, J.; Lu, F.; Luo, M.; Zhang, J.; Gao, H.; Wang, D.; Xing, W.; Jia, W.; Liu, F. The Efficacy and Safety of Cold Atmospheric Plasma as a Novel Therapy for Diabetic Wound In Vitro and In Vivo. *Int. Wound J.* 2020, 17(3), 851–863.
18. Kim, Y.J.; Lim, D.J.; Lee, M.Y.; Lee, W.J.; Chang, S.E.; Won, C.H. Prospective, Comparative Clinical Pilot Study of Cold Atmospheric Plasma Device in the Treatment of Atopic Dermatitis. *Sci. Rep.* 2021, 11(1), 14461.
19. Suwanchinda, A.; Nararatwanchai, T. Efficacy and Safety of the Innovative Cold Atmospheric-Pressure Plasma Technology in the Treatment of Keloid: A Randomized Controlled Trial. *J. Cosmet. Dermatol.* 2022, 21(12), 6788–6797.

20. Bekkers, V.Z.; Bik, L.; van Huijstee, J.C.; Wolkerstorfer, A.; Prens, E.P.; van Doorn, M.B.A. Efficacy and Safety of Needle-Free Jet Injector-Assisted Intralesional Treatments in Dermatology: A Systematic Review. *Drug Deliv. Transl. Res.* 2023, 13(6), 1584–1599.
21. Vanbever, R.; Pr at, V. In Vivo Efficacy and Safety of Skin Electroporation. *Adv. Drug Deliv. Rev.* 1999, 35(1), 77–88.
22. HIRONIC Co., Ltd. SYNERJET Pro – Medical Device for Aesthetics. Available from: <https://www.synerjetpro.com>.
23. Human Skin Clinical Trial Center Co., Ltd. Clinical Study Report: Evaluation of the Efficacy of Nano NMN 10% Ampoule Alone vs. Nano NMN 10% Ampoule with Synerjet on Facial Wrinkles (Crow’s Feet, Nasolabial Folds), Pores, Elasticity, Pigmentation Intensity, Pigmentation Area, and Deep Skin Hydration after 4 Weeks of Use. Protocol No.: HM-P25-0510. 2025.
24. Messaraa, C.; Metois, A.; Walsh, M.; Hurley, S.; Doyle, L.; Mansfield, A.; O’Connor, C.; Mavon, A. Wrinkle and roughness measurement by the Antera 3D and its application for evaluation of cosmetic products. *Skin Res. Technol.* 2018, 24(3), 359–366.
25. Park, H.S.; Shin, S. Clinical Efficacy and Safety Evaluation of a *Centella asiatica* (CICA)-Derived Extracellular Vesicle Formulation for Anti-Aging Skincare. *Cosmetics* 2025, 12(4), 135.
26. Bae, Y.; Son, T.; Nelson, J.S.; Kim, J.-H.; Choi, E.H.; Jung, B. Dermatological feasibility of multimodal facial color imaging modality for cross-evaluation of facial actinic keratosis. *Skin Res. Technol.* 2011, 17(1), 4–10.
27. Jung, G.; Kim, S.; Lee, J.; Yoo, S. Deep learning-based optical approach for skin analysis of melanin and hemoglobin distribution. *J. Biomed. Opt.* 2023, 28, 035001.
28. Van Nuffel, M.; Meulyzer, C.; Gheysen, B.; B hrer, A.; Anthonissen, M.; Van den Kerckhove, E.; Degreef, I. Palmar skin elasticity measured by the Cutometer MPA 580 is decreased in mild Dupuytren’s disease compared to healthy controls. *Hand Ther.* 2022, 27(1), 14–21.
29. Alves, P.L.M.; Nieri, V.; Moreli, F.C.; Constantino, E.; de Souza, J.; Oshima-Franco, Y.; Grotto, D. Unveiling New Horizons: Advancing Technologies in Cosmeceuticals for Anti-Aging Solutions. *Molecules* 2024, 29(20), 4890.
30. Venkatesan, K.; Dutta, G.; Bandyopadhyay, R.; Guha, N.; Debnath, B.; Manickam, S.; Sugumaran, A. Lipid nanocosmeceuticals: a novel approach to skin therapy for anti-aging and skin disorders. *Beni-Suef Univ. J. Basic Appl. Sci.* 2025, 14, 114.
31. Peng, T.; Chen, Y.; Hu, W.; Huang, Y.; Zhang, M.; Lu, C.; Pan, X.; Wu, C. Microneedles for Enhanced Topical Treatment of Skin Disorders: Applications, Challenges, and Prospects. *Engineering* 2023, 30, 170–189.
32. Mills, K.F.; Yoshida, S.; Stein, L.R.; et al. Long-Term Administration of Nicotinamide Mononucleotide Mitigates Age-Associated Physiological Decline in Mice. *Cell Metabolism* 2016, 24(6), 795–806.
33. Sinclair, D.A.; et al. Loss of Epigenetic Information as a Cause of Mammalian Aging. *Cell* 2023, 186(2), 305–326.e27.
34. Yi, L.; Maier, A.B.; Tao, R.; Lin, Z.; Vaidya, A.; Pendse, S.; Thasma, S.; Andrieu, N.; Dai, H.; Kumbhar, V. The efficacy and safety of β -nicotinamide mononucleotide (NMN) supplementation in healthy middle-aged adults: a randomized, multicenter, double-blind, placebo-controlled, parallel-group, dose-dependent clinical trial. *GeroScience* 2023, 45(1), 29–43.
35. Li, J.; Bonkowski, M.S.; Moniot, S.; Zhang, D.; Hubbard, B.P.; Ling, A.J.Y.; Rajman, L.A.; Qin, B.; Lou, Z.; Gorbunova, V.; Aravind L.; Steegborn C.; Sinclair D.A. A conserved NAD⁺ binding pocket that regulates protein-protein interactions during aging. *Science* 2017, 355(6331), 1312–1317.
36. Hakozaki, T.; Minwalla, L.; Zhuang, J.; Chhoa, M.; Matsubara, A.; Miyamoto, K.; Greatens, A.; Hillebrand, G.G.; Bissett, D.L.; Boissy, R.E. The Effect of Niacinamide on Reducing Cutaneous Pigmentation and Suppression of Melanosome Transfer. *Br. J. Dermatol.* 2002, 147(1), 20–31.
37. Tanno, O.; Ota, Y.; Kitamura, N.; Katsube, T.; Inoue, S. Nicotinamide Increases Biosynthesis of Ceramides as well as Other Stratum Corneum Lipids to Improve the Epidermal Permeability Barrier. *Br. J. Dermatol.* 2000, 143(3), 524–531.
38. Abella, M.L. Evaluation of anti-wrinkle efficacy of adenosine-containing products. *Int. J. Cosmet. Sci.* 2006, 28(6), 447–451.

39. Raszewska-Famielec, M.; Flieger, J. Nanoparticles for Topical Application in the Treatment of Skin Dysfunctions—An Overview of Dermo-Cosmetic and Dermatological Products. *Int. J. Mol. Sci.* 2022, 23(24), 15980.
40. Souto, E.B.; et al. Nanomaterials for Skin Delivery of Cosmeceuticals and Pharmaceuticals. *Appl. Sci.* 2020, 10(5), 1594.
41. Benson, H.A.E.; Grice, J.E.; Mohammed, Y.; Namjoshi, S.; Roberts, M.S. Topical and Transdermal Drug Delivery: From Simple Potions to Smart Technologies. *Curr. Drug Deliv.* 2019, 16(5), 444–460.
42. Roberts, M.S.; Mohammed, Y.; Pastore, M.N.; Namjoshi, S.; Yousef, S.; Alinaghi, A.; Haridass, I.N.; Abd, E.; Leite-Silva, V.R.; Benson, H.A.E.; et al. Topical and cutaneous delivery using nanosystems. *J. Control. Release* 2017, 247, 86–105.
43. Chen, X.; Zhu, L.; Li, R.; Pang, L.; Zhu, S.; Ma, J.; Du, L.; Jin, Y. Electroporation-enhanced transdermal drug delivery: Effects of logP, pKa, solubility and penetration time. *Eur. J. Pharm. Sci.* 2020, 151, 105410.
44. Kang, S.; Park, J.; Cho, E.; Kim, D.; Ye, S.; Jeong, E.T.; Jun, S.-H.; Kang, N.-G. Distinctive Gene Expression Profiles and Biological Responses of Skin Fibroblasts to Nicotinamide Mononucleotide: Implications for Longevity Effects on Skin. *Biomedicines* 2025, 13(10), 2395.
45. Hakozaiki, T.; Laughlin, T.; Zhao, W.; Deng, G.; Wang, J.; Moulton, L. Synergistic Effects of Niacinamide and Low pH on Melanin Synthesis, Melanocyte Function and Hyperpigmentation: In Vitro and Clinical Insights. *Int. J. Cosmet. Sci.* 2025, doi:10.1111/ics.70044.
46. Murugesan, M.; Mathiyalagan, R.; Ramadhania, Z.M.; Nahar, J.; Luu, C.H.; Phan, V.G.; Yang, D.C.; Zhou, Q.; Kang, S.C.; Thambi, T. Tailoring Hyaluronic Acid Hydrogels: Impact of Cross-Linker Length and Density on Skin Rejuvenation as Injectable Dermal Fillers and Their Potential Effects on the MAPK Signaling Pathway Suppression. *Bioact. Mater.* 2025, 49, 154–171.

Disclaimer/Publisher's Note: The statements, opinions and data contained in all publications are solely those of the individual author(s) and contributor(s) and not of MDPI and/or the editor(s). MDPI and/or the editor(s) disclaim responsibility for any injury to people or property resulting from any ideas, methods, instructions or products referred to in the content.